

Measurement of 2s and 3s Electron Spin Density in Iron Metal*

Cheng-yi Song,† Jan Trooster,‡ and N. Benczer-Koller
Rutgers, The State University, New Brunswick, New Jersey 08903

and

G. M. Rothberg
Stevens Institute of Technology, Hoboken, New Jersey 07030
(Received 17 July 1972)

The 2s and 3s electron spin densities at the nuclear site of ^{57}Fe in iron metal were measured by a new technique combining the Mössbauer effect with electron spectroscopy. Ratios $|\psi_{ns}^{\uparrow}(0)|^2/|\psi_{ns}^{\downarrow}(0)|^2 = 0.9937 \pm 0.0015$ and 1.012 ± 0.006 were measured for 2s and 3s shells, respectively. These results are in qualitative agreement with theoretical calculations of the core contributions to the magnetic hyperfine interaction.

The existence of large negative hyperfine fields in transition-metal ions has been successfully explained as due to polarization of core electrons¹: The exchange interaction between s-shell electrons and, in iron, the unpaired 3d electrons results in different s-electron radial wave functions, depending on whether the spin of the s electrons is parallel or antiparallel to the 3d magnetization. Consequently, there exists a net spin density $|\psi_{ns}^{\uparrow}(\vec{r})|^2 - |\psi_{ns}^{\downarrow}(\vec{r})|^2$ for each of the s shells of the atom, and in particular, a nonvanishing spin density at the nuclear site which results, via the Fermi contact interaction, in a hyperfine field at the nucleus. This core contribution to the hyperfine field can be written as the superposition of contributions from all the s-electron shells,

$$H_c = \frac{8}{3} \pi g \mu_0 S \sum_n [|\psi_{ns}^{\uparrow}(0)|^2 - |\psi_{ns}^{\downarrow}(0)|^2], \quad (1)$$

where g is the electron g factor, μ_0 is the Bohr magneton, S is the total spin of the ion, and the expression between brackets is the spin density at the nucleus of electrons in the ns shell, induced by one d -electron spin; n runs over all s shells to be considered. The total hyperfine field can be obtained experimentally by a variety of techniques such as ESR, NMR, or Mössbauer spectroscopy. These experiments, however, cannot distinguish the core contribution from those of other hyperfine interactions, such as the dipolar field of neighboring atoms and contributions from unquenched angular momenta. Moreover, H_c is a sum of contributions of opposite sign, each of which corresponds in turn to a small difference between large numbers. It is therefore desirable to measure the individual s-shell contributions to H_c as a test of the theoretical model and calculations.

In this experiment, use was made of the fact

that the probability α_{ns} for internal conversion of ns electrons is proportional to the ns -electron density $|\psi_{ns}(0)|^2$ at the nucleus.^{2,3} The $M1$ decay from the 14.4-keV, $I = \frac{3}{2}^-$, first excited state of ^{57}Fe to the ground state, $I = \frac{1}{2}^-$, proceeds mostly through internal conversion with a total internal conversion coefficient $\alpha = 8.17 \pm 0.25$.⁴ For an ^{57}Fe nucleus embedded in a ferromagnetic material, the direction of the 3d electron magnetization may be chosen as the quantization axis (Fig. 1). The nuclear transitions $\Delta m_I = 1$ ($m_{Ii} = -\frac{3}{2} \rightarrow m_{If}$

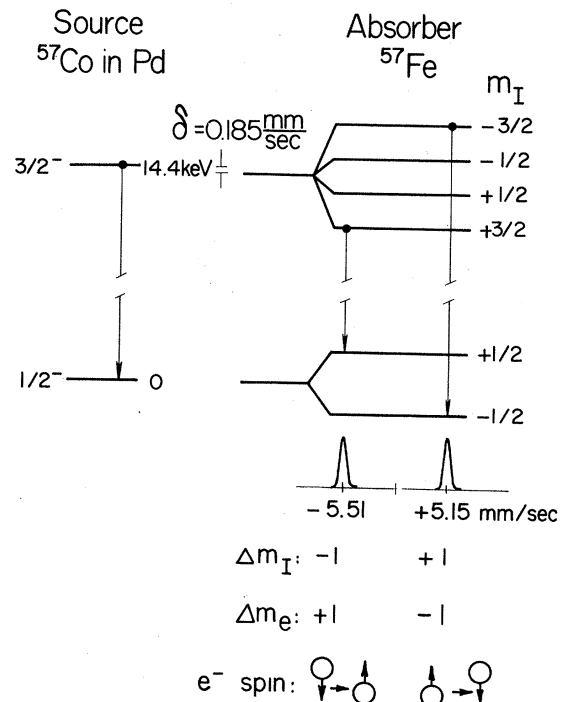


FIG. 1. Energy-level diagram of ^{57}Fe , indicating the $\Delta m_I = 1$ transitions, and the corresponding changes in angular momentum of the internally converted electrons.

$= -\frac{1}{2}$) and $\Delta m_I = -1$ ($m_{Ii} = \frac{3}{2} \rightarrow m_{If} = \frac{1}{2}$) correspond to total angular momentum changes of the emitted internal-conversion electron $\Delta m_e = -1$ and $\Delta m_e = +1$, respectively. If the electrons are emitted into a final s state $\Delta m_e = \Delta m_s$, where m_s is the z component of the spin angular momentum,

$$\alpha_{ns}(-\frac{3}{2} \rightarrow -\frac{1}{2}) \propto |\psi_{ns}^{\uparrow}(0)|^2,$$

$$\alpha_{ns}(\frac{3}{2} \rightarrow +\frac{1}{2}) \propto |\psi_{ns}^{\downarrow}(0)|^2.$$

Thus, the ratio $R = |\psi_{ns}^{\downarrow}(0)|^2 / |\psi_{ns}^{\uparrow}(0)|^2$ can be determined by measuring the ratio of internal-conversion electrons emitted in the decay of the $m_I = \pm \frac{3}{2}$ states separately for each of the four s shells of iron. The probability of emission into a final d state is less than 10% of the conversion into a final s state, and such processes were ignored.

A 92%-enriched ^{57}Fe absorber, $35 \mu\text{g}/\text{cm}^2$ thick and 1 cm diam, was prepared by evaporation on a lead-free microscope cover glass 0.1 mm thick. The iron film was annealed for 3 h at 450°C in a hydrogen atmosphere and placed at the source position of a solenoid magnetic β spectrometer. The $m_I = \pm \frac{3}{2}$ states of the ^{57}Fe nuclei were selectively excited by Mössbauer absorption of 14.4-

keV γ rays emitted by a 50-mCi ^{57}Co (Pd) source, with an active area of 2 mm diam. The source was mounted on an electromechanical drive and located at 2.75 or 4 mm behind the absorber. A lead collimator limited the diameter of the irradiated area of the absorber to 2 mm. A thin-window ($25 \mu\text{g}/\text{cm}^2$ Formvar) Geiger counter was used as the electron detector. The spectrometer field was set for transmission of any one of the K (6.3 keV), L_I (13.6 keV), or M_I (14.3 keV) + N_I (14.34 keV) electrons. The resolution of the instrument did not allow separation of the L_{II+III} , $M_{II\dots V}$, and N conversion electrons. However, their relative intensity is low [$L_I/L_{II+III} = 10.7$, $(M_I+N_I)/M_{II\dots V} = 13.4$, and $N_I/M_I = 0.034$].⁵ The final data were appropriately corrected for the effect of this unpolarized background.

The Mössbauer source was moved periodically in a constant velocity mode as depicted in Fig. 2(a). The source displacement corresponding to this velocity pattern is shown on Fig. 2(b). The electron counting rate was stored on a multichannel analyzer running synchronously with the drive wave form, Fig. 2(c). During $\frac{2}{3}$ of the period, the velocity corresponded to excitation of the $m_I = -\frac{3}{2}$ or the $m_I = +\frac{3}{2}$ levels, at $v = +5.15 \text{ mm}/\text{sec}$

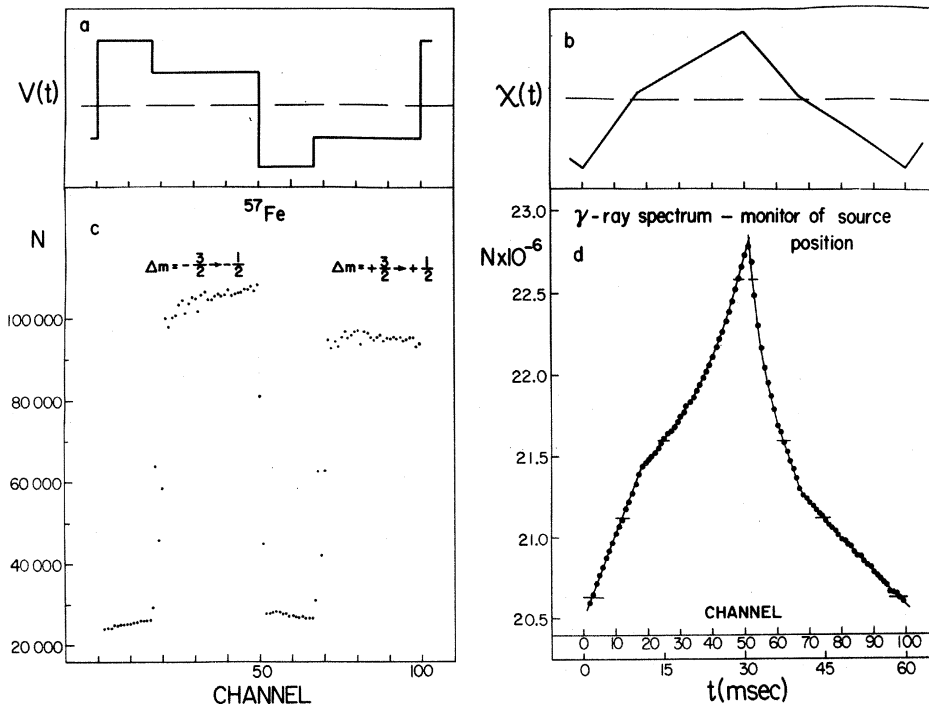


FIG. 2. (a) Reference wave form applied to the source drive, (b) corresponding source displacement, (c) electron spectrum obtained with the electron spectrometer set for detection of K electrons (total measuring time for this run was 89 h), and (d) spectrum of nonresonant radiation scattered from the absorber; channel intervals having the same source position are indicated by horizontal bars.

TABLE I. Measured spin density of s electrons at the nucleus in iron metal. $\delta_{ns} = |\psi_{ns}^\dagger(0)|^2 / |\psi_{ns}(0)|^2 - 1$.

		$10^2 \delta_{2s}$	$\delta_{3s} + \delta_{4s} \frac{ \psi_{4s}(0) ^2}{ \psi_{3s}(0) ^2}$ (%)	δ_{3s}^a (%)
Experiment	2.75 mm, 16.7 Hz	-0.62 ± 0.23	$+1.69 \pm 0.94$	
	2.75 mm, 8.3 Hz	-0.84 ± 0.30	$+1.14 \pm 0.99$	
	4.00 mm, 16.7 Hz	-0.39 ± 0.37		
	Average	-0.63 ± 0.15	$+1.43 \pm 0.68$	$+1.16 \pm 0.60$
Atomic wave functions, Refs. 1 and 6		-0.5		+2.0
Band theory, Ref. 7		-0.28		+1.0

^aA value of $\delta_{4s} \sim 8\%$ was chosen to extract the pure 3s contribution from the present experimental data. There is considerable disagreement both theoretical (Ref. 8) and experimental (Ref. 9) on the actual conduction electron polarization δ_{4s} .

and $v = -5.51$ mm/sec, respectively. The remaining time, the velocity was far from resonance and only background radiation was detected.

When comparing the internal-conversion rates from the $m_I = \pm \frac{3}{2}$ states, corrections have to be made for background and solid-angle effects. The background is due to cosmic rays and photoelectrons from external conversion of source γ rays in the absorber. The counting rate was strongly dependent on the displacement of the source because of the small source-absorber distance. To apply the proper background correction, it was therefore imperative to know the relative position of the source with high accuracy. To this end, the radiation scattered nonresonantly at about 90° by the absorber was monitored by two proportional counters placed in the plane of the absorber. The scattered intensity was stored in another multi-channel analyzer also synchronized to the wave form [Fig. 2(d)]. From these spectra it is possible to determine directly which "channels" correspond to the same source positions for the on- and off-resonant modes. Thus, the background in the on-resonance spectrum can be obtained from the measured off-resonance counting rate corresponding to the same source position. The background subtraction procedure was also checked by measuring electrons of energy higher than that of the M electrons. In this case, the background count was equal to the count obtained at the resonance velocity to an accuracy of $(0.08 \pm 0.13)\%$.

Since in all theoretical calculations the polarization effect in the 1s shell is of the order of $10^{-4}\%$, the background-corrected ratio of count-

ing rates at positive and negative velocities measured on the K electrons was used to normalize the ratios measured on the L_I and M_I electrons.

The measurements were carried out for drastically different geometries corresponding to two different source-absorber separations (2.75 and 4.0 mm) and two different frequencies (8.33 and 16.6 Hz). The results were in all cases in statistical agreement. The summary of these data is presented in Table I. We also show the theoretical predictions obtained either with atomic wave functions⁶ or from a band calculation.⁷

Finally, as a further test, measurements were also carried out on the decay of the $m_I = \pm \frac{1}{2}$ states. Because of admixture of $\Delta m_I = 0$ transitions, the polarization effect on the intensity ratio of the internal conversion is expected to be $\frac{1}{3}$ that observed for the decay of the $m_I = \pm \frac{3}{2}$ states. The observed effects were $\delta_{2s} = (-0.40 \pm 0.18)\%$ and $\delta_{3s} + \delta_{4s} [|\psi_{4s}(0)|^2 / |\psi_{3s}(0)|^2] = (0.52 \pm 0.64)\%$.

This experiment demonstrates the possibility of measuring individual s-shell spin densities at the nucleus by a new technique. In spite of considerable statistical errors due to the low efficiency of the particular β spectrometer used, it is nonetheless clear that the results support the theoretically predicted *sign* and *order of magnitude* of the spin polarization of the 2s and 3s electrons in iron.

We wish to thank Professor A. Freeman and Dr. R. Watson for many interesting discussions and their continuous encouragement. We also thank R. Tobin Fink for his help in the early stages of the experiment.

*Work supported by the National Science Foundation.

†Present address: Department of Physics, Purdue University, Lafayette, Ind. 47907.

‡Present address: Department of Physical Chemistry, Katholieke Universiteit, Nijmegen, Netherlands.

¹R. E. Watson and A. J. Freeman, Phys. Rev. **123**, 2027 (1961); A. J. Freeman and R. E. Watson, in *Magnetism*, edited by G. T. Rado and H. Suhl (Academic, New York, 1965), Vol. 2A.

²M. E. Rose, I. C. Biedenharn, and G. B. Arfken, Phys. Rev. **85**, 5 (1952).

³E. L. Church and J. Weneser, Ann. Rev. Nucl. Sci. **10**, 193 (1960); I. M. Band, L. A. Sliv, and M. B. Trzhaskovskaya, Nucl. Phys. **A156**, 170 (1970).

⁴W. Rubinson and K. P. Gopinathan, Phys. Rev. **170**, 969 (1968).

⁵F. T. Porter and M. S. Freedman, Phys. Rev. C **3**, 2285 (1971).

⁶P. S. Bagus and B. Liu, Phys. Rev. **148**, 79 (1966); M. Morita, K. Sugimoto, M. Yamada, and Y. Yokoo, Progr. Theor. Phys. **41**, 996 (1969).

⁷S. Wakoh and J. Yamashita, J. Phys. Soc. Jap. **35**, 1271 (1968).

⁸K. J. Duff and T. P. Das, Phys. Rev. B **3**, 2294 (1971).

⁹M. B. Stearns, Phys. Rev. B **4**, 4069 (1971), and private communication.

Bound Magnetic Polarons and the Insulator-Metal Transition in EuO[†]

J. B. Torrance, M. W. Shafer, and T. R. McGuire

IBM Thomas J. Watson Research Center, Yorktown Heights, New York 10598

(Received 14 August 1972)

A new model is presented for the insulator-metal transition in Eu-rich EuO: At low temperatures the electrons are only very weakly bound to oxygen vacancies and conduction is metallic; near and above T_c the electrons *localize* and form bound magnetic polarons by ordering the Eu²⁺ spins neighboring the vacancy, thereby gaining exchange energy. Magnetic-susceptibility data are presented which support this model.

The conductivity behavior typical of Eu-rich EuO is shown by the solid curve in Fig. 1. As the temperature is lowered below 300 K, the conductivity decreases with an activation energy of typically 0.3 eV, similar to an ordinary semiconductor. Between 120 and 70 K the conductivity is too low to be measured. However, below the ferromagnetic ordering temperature of 69 K, the conductivity suddenly increases by more than 13

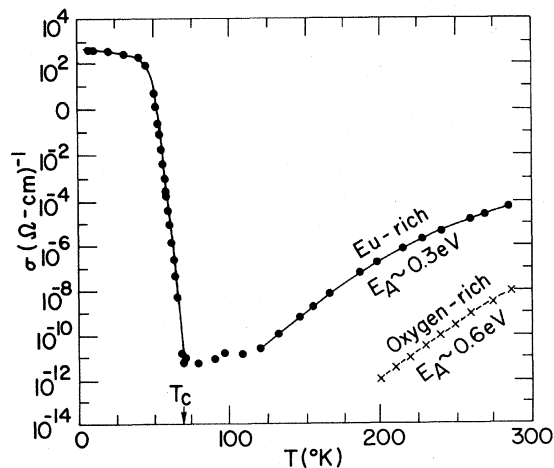


FIG. 1. Conductivity of Eu-rich EuO (after Ref. 5) and oxygen-rich EuO (after Ref. 7).

orders of magnitude and becomes nonactivated, or metallic, below 50 K. This insulator-metal transition was first discovered by Oliver¹ and has since been examined by a number of authors.²⁻⁷ For comparison, the dashed curve in Fig. 1 is the conductivity for an oxygen-rich sample, which has an activation energy of typically 0.6 eV and shows no insulator-metal transition.⁷ Therefore, the transition is not intrinsic in origin, but involves the extra electrons in Eu-rich EuO, which are presumably associated with oxygen vacancies.^{1,4,7} In this Letter we propose a new explanation for the insulator-metal transition in EuO^{8,9} and present new magnetic-susceptibility data which favor this model over earlier models.

Oxygen vacancies hold two electrons and, hence, are much more complicated than one-electron donors. The basic assumption and the new feature of the model described here, the bound magnetic polaron (BMP) model, is that oxygen vacancies in EuO are *shallow* donors, as in CdO,¹⁰ ZnO,^{11,12} and possibly BaO.¹³ This implies that one of the electrons is loosely bound. In this paper we shall concentrate on the effects of this electron and neglect the other, more tightly bound electron. Thus, the ground state in